

Structural modification of phenoxyimine titanium complexes and activation studies with alkylaluminum compounds

Huaqin Yang,^[a, b] Yara van Ingen,^[b, c] Burgert Blom,^[c] Sanjay Rastogi,^[a, b] and Dario Romano*^[a, b]

The synthesis and characterization of three complexes of the type (N-(3-*tert*-butylsalicylidene)-R)₂TiCl₂ [R = 2,6-difluorophenyl **1**, R = 2,6-dimethylphenyl **2**, R = phenyl **3**] is reported and compared with the highly active R = 2,3,4,5,6-pentafluorophenyl **4**. The complexes were tested for ethylene polymerization when activated with different co-catalysts, giving high catalytic activity when activated with methylaluminumoxane for complexes **3** and **4**. Complex **3** is the only catalyst to be inactive when activated with diethylaluminum chloride. Unexpectedly, for complexes **1** and **2**, no catalytic activity is recorded when butylated hydroxytoluene in methylaluminumoxane is used to remove the trimethylaluminum, while the catalytic activity for complex **3** is retained. NMR study on the activation of the four

complexes in the presence of common alkyl aluminum co-catalysts suggests the formation of Ti(III) species in the presence of tri-*iso*-butylaluminum, and also the formation of NR-CH₂ (R: -Al(CH₂CH(CH₃)₂)₂) bond from the N=C-H bond of the ligand explaining the absence of catalytic activity. Density functional theory calculations using B3LYP and a combination of basis sets (6-31+G and cc-pVTZ) were performed on the catalyst precursors and the activated species showing insights into the frontier orbitals, localizing the LUMO on the imino bond elucidating their reactivity. Mulliken charges are also reported and an unexpected relationship between the nitrogen on the ligands and the molecular weight is observed.

1. Introduction

Bis(phenoxyimine) ligands bound to early transition metals (mainly group (IV)) (also known as FI complexes, Figure 1), developed by Fujita and co-workers, belong to a family of catalyst precursors highly active in olefin polymerization.^[1] Activated FI complexes show unprecedented catalytic activities for ethylene polymerization, displaying significant higher activities compared to metallocene catalysts.^[2-5] Most studies focus on the modification of positions R₁ and R₃ which are

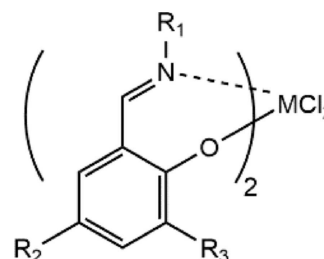


Figure 1. Generic structure of the FI catalysts. M=Ti, Zr, Hf.

considered to be responsible for their activity during polymerization and the resulting molecular characteristics of the polymers produced; while R₂ does not show a significant influence neither on the activity nor the molecular weight (M_w) of polymer.^[1-2,6-7] In particular, Matsui and co-workers used different alkyl groups (methyl, *iso*-propyl, and *tert*-butyl) at the R₃ position of bis(phenoxyimine) zirconium (FI-Zr) complexes to synthesize polyethylene. They found that the steric effect of the R₃ group significantly influences the polymerization activity, but not the polymer's M_w . When the highest sterically demanding group is employed (*tert*-butyl) the highest activity is recorded while for other groups similar M_w are measured.^[8] Subsequently, they studied FI-Zr complexes with different alkyl groups (aniline phenyl, 1-methyl phenyl, 1-*iso*-Propyl phenyl) at the R₁ position for synthesizing polyethylene. They found that by increasing the steric demand of R₁ resulted into higher M_w , attributing the reduction of the β -hydrogen (β -H) chain transfer to the steric repulsion between the alkyl group and the β -H on

[a] H. Yang, Prof. S. Rastogi, Dr. D. Romano

Department of Biobased Materials

Faculty of Science and Engineering

Maastricht University

Brightlands Chemelot Campus

Geleen 6167 RD (The Netherlands)

E-mail: dario.romano@maastrichtuniversity.nl

[b] H. Yang, Y. van Ingen, Prof. S. Rastogi, Dr. D. Romano

Aachen-Maastricht Institute for Biobased Materials

Brightlands Chemelot Campus

Geleen 6167 RD (The Netherlands)

[c] Y. van Ingen, Dr. B. Blom

Maastricht Science Programme

Faculty of Science and Engineering

Maastricht University

Kapoenstraat 2

PO Box 616

6200 MD, Maastricht (The Netherlands)

Supporting information for this article is available on the WWW under <https://doi.org/10.1002/cctc.202000731>

© 2020 The Authors. Published by Wiley-VCH GmbH. This is an open access article under the terms of the Creative Commons Attribution License, which permits use, distribution and reproduction in any medium, provided the original work is properly cited.

the growing chain. This indicated that M_w depends on the bulkiness of the R_1 substituents.^[2] Mitani *et al.* synthesized bis(phenoxyimine) titanium (FI-Ti) complexes with varying number and positioning of fluorine atoms (F) on the N-phenyl group R_1 . They found that the increasing number of F in R_1 group induce higher catalytic activities, which is likely due to the increasing electron-withdrawing effect of F resulting in a more electrophilic Ti center. Additionally, the F can interact with the β -H of the growing polymeric chain, effectively destabilizing the transition state leading to the β -H transfer.^[7] Furthermore, Iwashita and co-workers applied fluorinated moieties of R_1 to study the non-covalent attractive interaction for the active species. A $M\cdots F\cdots C$ interaction has been proposed to account for the remarkable effects of F in the related catalytic systems. Such interactions could conceivably stabilize a highly electron-deficient metal center, which is subject to facile deactivation and disfavor chain transfer processes.^[9] Similarly, Marks and coworkers applied 3,5-bis(trifluoromethyl)phenyl and 3,5-(dimethyl)phenyl in the *ortho* positions on group R_1 with mono^[10] and bimetallic nickel^[11] for ethylene polymerization, and they found that there is non-negligible $C_\beta\text{---}H_\beta\cdots F(C)$ through-space dipolar interactions and $C\text{---}F\cdots H\text{---}C$ interaction disfavors the chain transfer. Hence, the F in the *ortho* positions suppress the β -H chain termination mechanism and allow the synthesis of ultra-high molecular weight polyethylene. Often, the electronic and steric effects are de-coupled and studied separately. A systematic study on the steric effects, coupled with the electronic effects (including a study of the frontier orbitals), seems to have escaped the attention.

Varying the combination of complexes and co-catalysts result in very different catalytic activities, M_w and polydispersity indexes (PDI) of the polymers.^[12–13] Common co-catalysts include alkylaluminum compounds such as trimethylaluminum (TMA), triethylaluminum (TEA), tri-*iso*-butylaluminum (TiBA) and diethylaluminum chloride (DEAC). This class of co-catalysts have the advantage of, in addition to catalyst activation, scavenging impurities prior to the introduction of the catalyst system to the medium.^[14] However, it was observed that such alkylaluminum co-catalysts were more active for heterogeneous Ziegler-Natta based catalysts than metallocenes, likely due to the a strong interaction with the metal center (upon activation) and the possibility to modify the structure of the ligand, in metallocenes.^[12,15] For metallocene activations, methylaluminoxane (MAO) and borate co-catalysts have been found to be most efficient compared to alkylaluminum. Where MAO involves the abstraction of a halide from the metal center, generally $-Cl$, and borates abstract an alkyl group, generally $-CH_3$. Due to its large size (weak interaction with the positively charged activated catalyst), strong Lewis acidity and weak reduction ability, MAO and modified methylaluminoxane (MMAO) are commonly employed co-catalysts for Ti(IV) systems, including the FI complexes.^[16] Scattered information on the use of FI-Ti complexes using different co-catalyst can be found in literature. Therefore, understanding the chemistry/interactions between the two components is of critical importance. However, a systematic study on the steric and electronic effect coupled with the activation capability of a series of catalyst

activators having different Lewis acidity is missing. Hence, the variation of the co-catalysts' Lewis acidity is taken into account in this study.

Normally, MAO is used as a co-catalyst for the oligomerization and polymerization of a variety of monomers.^[17–18] Despite a wide use of MAO in olefin polymerization, its exact structure and composition is still unclear.^[14,18–19] MAO is synthesized by controlled hydrolysis of TMA and therefore contains a significant amount of TMA residue,^[20] which influences many catalytic systems, including FI complexes.^[21] Makio and Fujita used ¹H NMR to study the formation of the active species of bis[N-(3-*tert*-butylsalicylidene)-2,3,4,5,6-pentafluoroanilinato] Ti(IV) dichloride (complex 4) when activated with MAO. They found that the presence of TMA can react with the active species $[L_2TiMe]^+$ forming an inactive species $[L_2TiMe]^+MeAlMe_2$ ($L=N$ -(3-*tert*-butylsalicylidene)-2,3,4,5,6-pentafluoroanilinato).^[22] Moreover, Konstantin and co-workers found that the active species from complex 4 and MAO/TMA catalytic system is an outer-sphere ion pair, $[L_2TiMe]^+[Me\text{---}MAO]^-$. The $[Me\text{---}MAO]^-$ anion can decompose at 20 °C in toluene with a half-life of 1 h which reacts with the active species forming $L_2Ti(III)Me$ or $LAIME_2$.^[23] To avoid the influence of the TMA on the catalytic system, a co-catalyst modifier, namely 2,6-di-*tert*-butyl-4-methylphenol (BHT), can be used in combination with MAO to scavenge the free TMA in solution.^[24] Our research group showed that the use of BHT in combination with MAO and other MMAOs improve the catalytic activity toward the polymerization of ethylene for complex 4.^{[14][21]} However, the use of BHT is limited to very few catalytic systems. In this article, we aim to acquire additional experimental data and relationship on the influence of different co-catalysts (including a modifier) on the activation ability of the FI-Ti catalyst precursors.

This research studies the activation of four different types of FI-Ti complexes having different ligands in position R_1 with and without F and their ability to promote the polymerization of ethylene when activated with different co-catalysts (MAO, MAO/BHT, DEAC, DEAC + MAO/BHT). The four complexes are bis[N-(3-*tert*-butylsalicylidene)-2,6-difluoroanilinato] Ti(IV) dichloride (complex 1), bis[N-(3-*tert*-butylsalicylidene)-2,6-dimethylanilinato] Ti(IV) dichloride (complex 2), bis[N-(3-*tert*-butylsalicylidene)-anilinato] Ti(IV) dichloride (complex 3), bis[N-(3-*tert*-butylsalicylidene)-2,3,4,5,6-pentafluoroanilinato] Ti(IV) dichloride (complex 4). The complexes were chosen due to their different electron and steric natures in order to study the influence on the catalytic activity toward ethylene polymerizations and M_w of the resulting polymers. The difference in Lewis acidity of the four different co-catalysts is also taken into account and used to understand in more detail their activation ability. Complex 4 is unreactive in the presence of alkylaluminum such as TiBA,^[16] and an interest is stimulated in the reactivity of other synthesized complexes with such co-catalysts. The nuclear magnetic resonance (NMR) study of the activity of the synthesized complexes with different alkylaluminum co-catalysts (TEM and TiBA) by different Al/Ti ratio is also reported. DFT analysis on the catalyst precursors and the activated species is performed and the frontier orbitals, together with the Mulliken

charges, are correlated with the molecular weight and reactivity of the catalyst precursors with the co-catalysts.

Experimental Part

Materials

All manipulations of air and moisture-sensitive compounds were performed under nitrogen (N_2) atmosphere, using Schlenk-techniques or in a glovebox, unless stated otherwise. Aniline, *n*-Butyl lithium, anhydrous diethyl ether, anhydrous hexane, 2,6-difluoroaniline and titanium(IV) chloride were purchased from Sigma Aldrich. Anhydrous toluene and anhydrous THF were purchased from LPS and further purified using MBraun compact solvent purifier systems. *p*-toluenesulfonic acid, pentafluoroaniline, 2,6-dimethylaniline and 3-*tert*-butylsalicylaldehyde were purchased from Acros. $CDCl_3$ and C_6D_6 were purchased from Cambridge Isotope Laboratories and dried over molecular sieves. Dichloromethane was saved in molecular sieves for use. MAO was purchased from Albemarle. TEA, TIBA and DEAC were purchased from Sigma Aldrich. All other chemicals were used as received.

Ethylene polymerization

The polymerization was conducted in a Büchi 1.5 L metal reactor vessel, equipped with thermometer probe, gauge, injection switch, solvent inlet, gas and vacuum pipes, Büchi stirrer with a three-blade-propeller. Using a Huber Unistat 430w thermostat, the reactor was heated to 125 °C overnight under vacuum. Afterwards, the reactor was filled with N_2 and vacuum/ N_2 cycles were performed at least three times. After the vacuum/ N_2 cycles, the temperature was brought to the operating temperature and 750 ml of anhydrous toluene were added to the reactor under a constant stirring set and controlled at 750 rpm using a Büchi cyclone 300. The solvent temperature was set and controlled to 10 °C. After temperature equilibration was achieved, the N_2 was then replaced with 1.1 bar absolute pressure of ethylene by means of a press flow gas control unit BPC6002.

80% vol./vol. of the co-catalyst was introduced into the reactor as scavenger for removing the impurities. 20% vol./vol. of the co-catalyst was mixed with 4 ml of anhydrous toluene. In the glovebox, 14 μ mol of complex were dissolved with the previously mixed co-catalyst and toluene and injected in the reactor and the monomer pressure was quickly raised to 2.0 bar absolute pressure. All polymerizations were performed with a ratio of Al/Ti=1000. After 60 min, the polymerization was stopped by releasing the monomer and injecting 5–10 ml of Ethanol. The polymer was then discharged in a beaker containing acidified ethanol (~50 mL) and, after few minutes, the polymer was filtered, washed with copious amounts of ethanol and acetone and dried in vacuum at 40 °C until constant weight.

Polymerization with MAO

80% vol./vol. of MAO (7.45 mL of a 10 wt% solution in toluene) was injected as scavenger. 14 μ mol of complex was dissolved in 4 mL of toluene and activated with 20% vol./vol. of MAO (1.8 mL of a 10 wt% solution in toluene). The polymerization conditions were shown as before.

Polymerization with MAO/BHT

BHT (3.68 mmol, 0.81 g) was added to MAO (9.32 mL of a 10 wt% solution in toluene) in a Schlenk vial in the glovebox and stirred for 30 min. 80% vol./vol. of this co-catalyst solution (7.45 mL, BHT + MAO) was introduced as a scavenger to the reactor and the nitrogen stream was replaced with ethylene gas. 14 μ mol of complex was dissolved in 4 mL of toluene with the remaining 20% vol./vol. of the co-catalyst solution, in the glovebox. The polymerization conditions were shown as before.

Polymerization with DEAC

80% vol./vol. of DEAC (97% sol., 11.1 mmol, 1.29 mL) was added to the reactor as scavenger and allowed to react for 15 min. The remainder 20% vol./vol. of DEAC (2.7 mmol, 0.32 mL) was added to 14 μ mol of complex as activator with 4 mL of toluene. The polymerization conditions were shown as before.

Polymerization with DEAC and MAO/BHT

Co-catalyst combination (Al/Ti=1000) was made by scavenger 80% mol./mol. DEAC (11.1 mmol, 1.29 mL) and activator consisting of 10% mol./mol. pre-reacted for 30 min MAO/BHT and 10% mol./mol. DEAC (1.35 mmol, 0.16 mL). BHT (0.38 mmol, 0.83 g) was added to MAO (10 wt% sol. in toluene, 1.44 mmol, 0.932 mL) under stirring for 30 min to remove TMA impurity. 80% mol./mol. of DEAC was added to the reactor as a scavenger and allowed to react for 15 min. The activator solution was made through addition of DEAC (1.39 mmol, 0.16 g) to the MAO/BHT mixture and 14 μ mol of complex. Upon injection of this activator solution, the polymerization was initiated. The polymerization conditions were shown as before.

Characterization

Density functional theory calculations

DFT calculations were performed to model complexes **1**, **2**, **3** and **4**. The Gaussian09 W Revision E.01 software package was used. The software package Gaussian09 was employed for visualization, analysis and editing of input, checkpoint and output files.^[25] The level of theory used for all calculations is B3LYP with the basis set 6-31+G for H, C, N, O, F and Cl atoms. Whilst for Ti the cc-pVTZ basis set was used to ensure more accurate representation of the d-orbitals. Geometry optimizations were calculated without any constraints. All the optimized geometries showed non imaginary frequency. Distorted octahedral geometries having the two oxygens in trans-position and two chlorines in cis-position is inputted according to previous x-ray crystallographic analyses.^[7]

¹H NMR measurements

NMR tubes were equipped with a J. Young valve to allow sample preparation and measurement under N_2 atmosphere. The desired amount of complex (~45 mg) was weighed and transferred into the NMR tube. The corresponding alkylaluminum volume was taken up by syringe and injected into the tube, along with sufficient C_6D_6 up to a total volume of 0.7 mL under nitrogen flow. The J. Young valve was secured on the tube and brought out for immediate measurement.

DSC measurements

1.5 mg ± 0.5 mg of polymers were weighed in high precision TA instruments T-zero aluminum pan and lid. TA instruments DSC250 was used to perform the measurement under N₂ atmosphere at a constant flow of 50 mL/min.

A heating ramp was imposed to the sample starting from 50 °C to 160 °C at 10 °C/min, followed by a cooling rump to 50 °C at 10 °C/min; these two ramps are repeated twice per each polymer characterized. The melting temperature and crystallinity of the polymers were obtained from the first heating cycle. A calibration using Indium is applied.

FT-IR measurements

The FT-IR machine used was a Shimadzu MIRacle 10 coupled with an attenuated total reflection accessory for measuring solid samples. A small amount of sample is carefully deposited on the diamond window and the analysis is performed. The parameters of the analysis were the following: 64 scans, resolution: 2 cm⁻¹, apodization: Happ-Genzel.

Hot compaction

To the nascent polymer powder, 0.7–1.0 wt% of Irganox 1010 (weight percentage in polymer) was added and dissolved in acetone. Afterwards, the acetone is let dry. Irganox 1010 is added to prevent thermal degradation of the polymer during the long rheological measurements in the melt. Approximately 0.13 g of polymer were compressed in a 12 mm metal mould for 5 min at 10 bar, 10 min at 50 bar, 5 min at 100 bar at 125 °C in a DrCollin P200 hot press to obtain 12 mm discs.

Rheological analysis

The 12 mm polymer disc was placed in between two parallel plates of 12 mm at an initial temperature of 110 °C using a TA Instrument Discover Hybrid Rheometer 1. The temperature was regulated by a convection oven under constant N₂ flow. Following thermal stabilization at 110 °C, the temperature was increase to 130 °C at 10 °C/min under a constant strain of 0.1%, constant compression force of 1 N and fixed oscillation frequency of 10 rad/sec. After thermal stabilization, the sample was heated further to 160 °C at 10 °C/min under a constant strain of 0.1%, constant compression force of 4 N and fixed oscillation frequency of 10 rad/sec. From this point forward, a constant compression force of 4 N was applied throughout the remaining rheological tests. Once 160 °C were reached, 90 seconds for the temperature stabilization are waited. From this point ongoing, a fixed temperature of 160 °C was maintained throughout all the further rheological measurements. An oscillation amplitude was performed from 0.05 to 1.5% of strain at fixed oscillation frequency of 10 rad/sec to establish the linear viscoelastic regime. Subsequently, an oscillation time sweep test was performed applying a strain within the viscoelastic regime (typically 0.1–0.3%) at fixed oscillation frequency of 10 rad/sec to equilibrate the sample. Once the polymer reaches the equilibrium (the storage modulus does not change in time), a second oscillation amplitude was performed to check the linear viscoelastic regime, followed by an oscillation frequency sweep test using values of strain within the linear viscoelastic regime and scouting values of oscillation frequency from 600 rad/sec to as low as 10⁻³ rad/sec.

To estimate M_w and the PDI of the polymers, the commercial TA Instrument Orchestrator software based on the computational method developed by mead was used by fitting the viscoelastic

functions (storage (G') and loss (G'') moduli) as a function of oscillatory frequency.^[26]

2. Results and Discussions

2.1. Ligand and Complex Synthesis

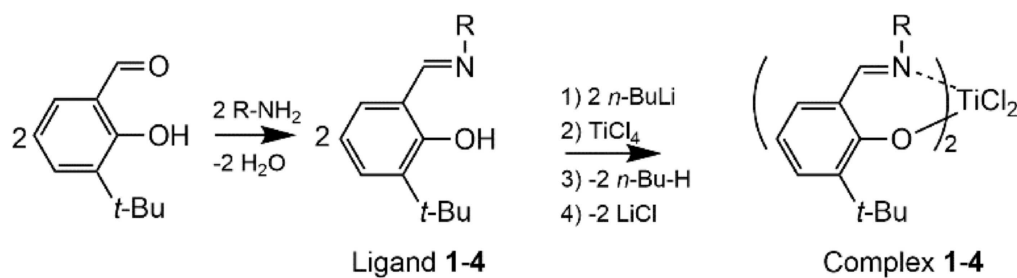
The synthetic method of bis(phenoxyimine ligand) titanium dichloride is shown in Scheme 1.

The first step of the reaction follows a Schiff-base mechanism, where the aldehyde carbonyl bond (C=O) reacts with a primary amine forming an imine bond (C=N) with elimination of water, as seen in Scheme 1, forming ligands **1**, **2**, **3** and **4**. This steps requires separation of unreacted products by column chromatography. The yield of phenoxyimine ligands are 15%, 20%, 35%, 58%, for ligands **1**, **2**, **3** and **4** respectively, which are lower than the literature^[7] (82–98%) due to the loss of product in the separation by column chromatography. N-(3-*tert*-butylsalicylidene)-2,6-difluoroaniline, N-(3-*tert*-butylsalicylidene)-2,6-dimethylaniline, N-(3-*tert*-butylsalicylidene)-aniline, N-(3-*tert*-butylsalicylidene)-2,3,4,5,6-pentafluoroaniline were synthesized followed the reference.^[3,7,27]

LC–MS data (Figure S1–3) shows the main m/z signals to correlate to a mass of 290 g/mol, 282 g/mol, 254 g/mol and 344 g/mol respectively for ligands **1**, **2**, **3** and **4**, corresponding to 1 g/mol higher than the synthesized product due to ionization. The C=O stretching vibration in the IR spectrum (Figure S30–32) of the starting aldehyde at 1647 cm⁻¹ moves to 1622 cm⁻¹ (ligand **1**), 1612 cm⁻¹ (ligand **2**), 1603 cm⁻¹ (ligand **4**), representing the formation of a C=N bond. This indicates the completion of the reaction and formation of a pure final product. Furthermore, in the purified product no indication of starting material could be seen, whilst this was visible in the MS analysis of the crude product. The ¹H NMR characterization of the ligands (Figure S4, S7, S9, S11) show no impurities and match the expected signals.

The second step in complexes formation, follows the reaction of 1 eq. of TiCl₄ with 2 eq. of the synthesized phenoxyimine ligands in dried diethyl ether, previously initiated by deprotonation of the hydroxyl using *n*-buthyllithium, forming a lithium salt of the ligand and *n*-butane. The two negatively charged phenoxy ligands substitute two Cl⁻, and the nitrogens on the imine form a coordinate bond with Ti, giving the complex and LiCl. The synthesized products show the good yield, 50%, 90%, 42%, 29% for complexes **1**, **2**, **3** and **4** respectively. The NMR results show that the characteristic peaks of H (OH, ligand, $\delta = 13.6$ –13.8 ppm) disappear from catalyst ¹H NMR spectrums (Figure S13, S16, S18, S20), which suggests the complexation between the OH group and metal center Ti.

Additional details and characterization of the intermediate ligands and the complexes can be found in the supporting information.



R:				
Ligand	1	2	3	4
Yield (%)	15	20	35	58
Complex	1	2	3	4
Yield (%)	50	90	42	28

Scheme 1. Reaction scheme and yields for the synthesis of complexes 1, 2, 3 and 4.

2.2. Density Functional Theory (DFT) Studies

In order to gain an insight on the electronic parameters of the complexes, the four complexes and their respective cationic mono-alkylated species (active species) are modelled using DFT. Table 1 summarizes relevant Mulliken charges for the complexes and the activated forms.

From the values reported in Table 1, the two sets of Mulliken charges for the nitrogen and carbon are practically identical reflecting the C_2 symmetric nature of the catalyst precursors. However, in the case of the activated species, small differences in the Mulliken charges are found between the same atoms of the two ligands. The values of the Mulliken charges for the nitrogen and carbon change upon activation, reflecting the vicinity with the positively charged titanium. On the contrary, the Mulliken charges for the *ortho*-atoms do not

significantly change upon activation, reflecting the larger distance to the titanium.

Figure 2 shows the optimized structures of complexes 1, 2, 3 and 4 obtained from DFT computations. The optimizations show a distorted octahedral structure, agreeing with the previously published elucidations from X-ray crystallography by Mitani *et al.*^[7] In particular, it is of importance to remark that the structure of complex 2, containing dimethyl in the ligand framework, is indistinguishable from the fluorine-containing complexes. This indicates the equivalence in steric effect of the two groups and the little influence the electronic nature of the fluorine has on the structural spacing of the atoms. The *cis*-location of the Cl leaving groups are clearly seen. The *cis* configuration of leaving groups, once replaced by alkyl groups and later active polymerization sites, are known to be imperative for high polymerization rates.^[3,7] Figure S58 shows

Table 1. Selected Mulliken charges of the four complexes and the active species calculated using DFT.

Catalyst	Mulliken Charges		Immine C		<i>ortho</i> -atom ^[a]		
	N						
1	0.508	0.508	-0.158	-0.158	<i>o</i> -F:	-0.210	-0.202
2	0.203	0.202	-0.160	-0.159	<i>o</i> -H:	0.204	0.264
3	0.048	0.048	-0.167	-0.167	<i>o</i> -H:	0.188	0.208
4	0.534	0.534	-0.242	-0.242	<i>o</i> -F:	-0.180	-0.175
1-act.	0.361	0.345	0.294	0.265	<i>o</i> -F:	-0.229	-0.171
2-act.	0.369	0.268	-0.215	-0.276	<i>o</i> -H:	0.217	0.231
3-act.	0.063	-0.014	0.101	0.098	<i>o</i> -H:	0.186	0.201
4-act.	0.441	0.393	-0.090	-0.065	<i>o</i> -F:	-0.203	-0.146

[a] Indicating the most negative and the most positive fluorine in positions 2 and 6 for complexes 1 and 4 or the most negative and the most positive hydrogen in complexes 2 and 3; in the case of complex 2 is considered the hydrogen on the methyl.

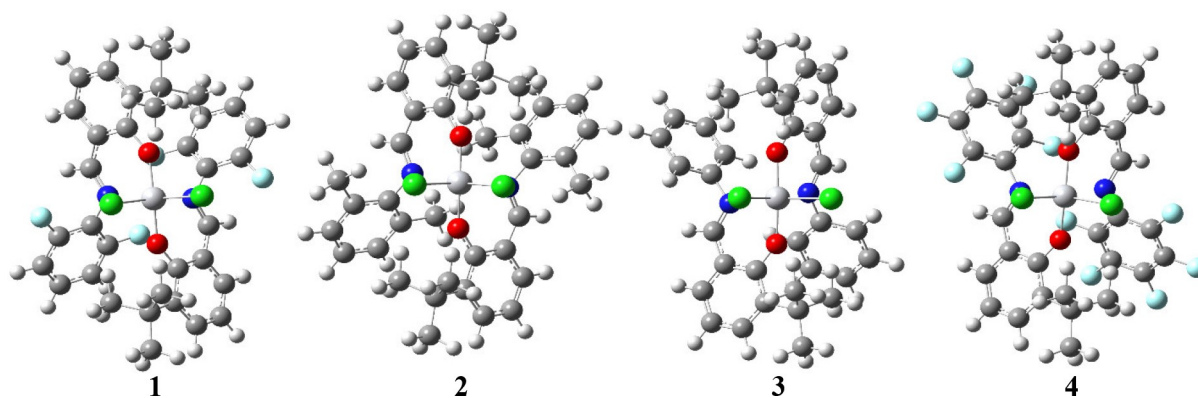


Figure 2. DFT Optimized structures of complexes 1, 2, 3 and 4.

the optimized structures of the active species of complexes 1 to 4. The obtained geometries are distorted trigonal bipyramids as expected from the penta-coordination of the titanium metal center.

Calculations of the highest occupied molecular orbital (HOMO) and lowest unoccupied molecular orbital (LUMO) energies are depicted in Figure 3.

The HOMO and LUMO values of complexes 1 and 2 are nearly equivalent, indicating little effect of the electronic nature of the fluorine on the molecular orbitals. The increased number of fluorine in complex 4 does however decrease the HOMO and LUMO energies slightly.

The HOMO is regarded as e^- donating and nucleophilic, whilst the LUMO as e^- accepting and electrophilic. It can be seen that the HOMOs of the four complexes are located on very similar places of the structures, focused for a majority on the aromatic rings, oxygens and chlorines where most of the electron density is located. The localization of the HOMO on the chlorine reflects the likelihood of exchanging one chlorine with an alkyl group in the presence of a co-catalyst activator. It can be speculated that the tendency of the ligand transfer to the extremely electron poor TMA observed in previous findings can be justified by the presence of the HOMO delocalized on the nitrogen and oxygen.^[15,28–29] The LUMOs of the four complexes

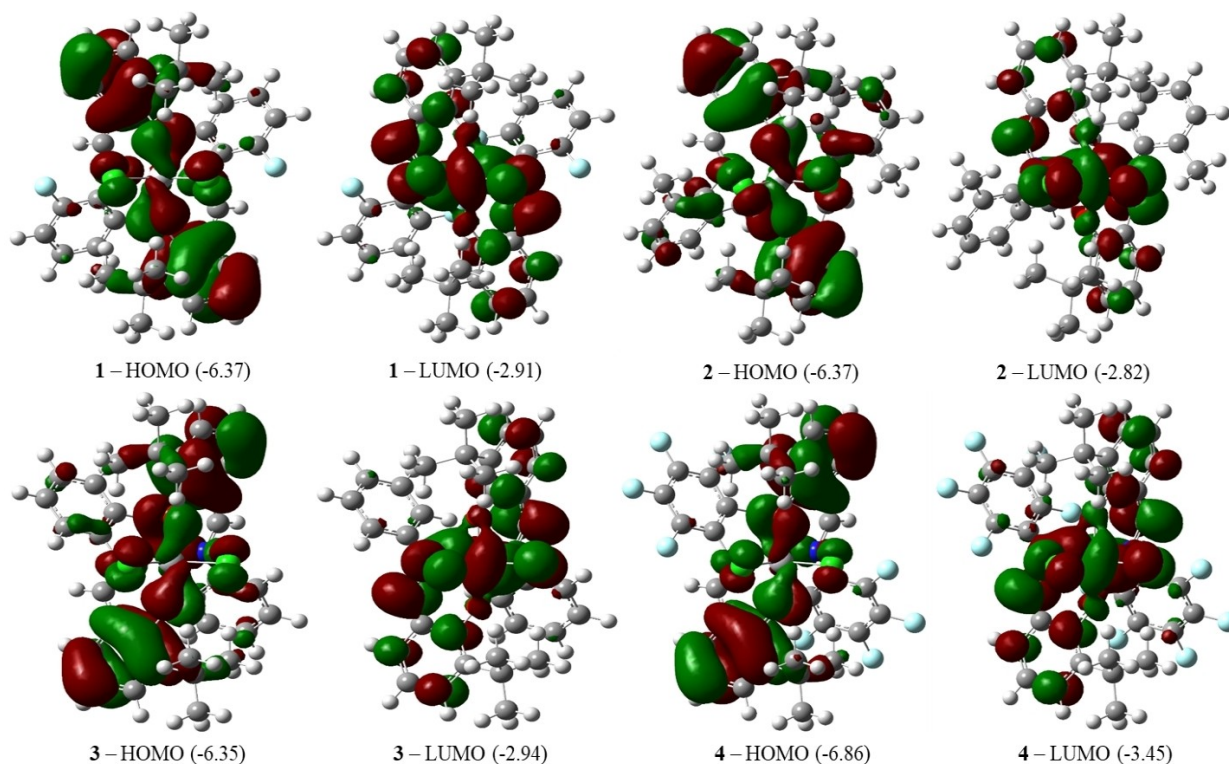


Figure 3. HOMO and LUMO visualizations of complexes 1, 2, 3 and 4. Energies are expressed in eV.

are relatively similar and are primarily located on the imido and the Ti–Cl bonds. This suggests that a nucleophile will preferably react with the imido or Ti–Cl bonds. The effect of the presence of the electron attracting fluorines in complexes 1 and 4 is visible in the Mulliken charges calculated on the nitrogen. In particular, the most electron withdrawing group on the nitrogen belongs to complex 4 which shows the highest charge; while the most electron donor group on the nitrogen belongs to complex 3 which shows the lowest charge. Moreover, the Mulliken charges of the atoms in *ortho* positions are negative only for the fluorines of complexes 1 and 4 while for complexes 2 and 3 the Mulliken charge on the hydrogens are positive. This indicates that only the fluorines will be available for an electrostatic interaction with the positively charged titanium (upon activation) and/or the β -hydrogen on the growing chain.

The frontier orbitals of the activated species of complexes 1 to 4 can be found in Figure S59. The HOMOs of the active species of complexes 1 to 4 are delocalized on the phenoxy-aromatic rings of the ligands and the oxygens. The LUMOs of the active species of complexes 1 to 4 are mainly delocalized on the positively charged titanium and the imido bond (mainly on the carbon). Some differences can be appreciated between the size of the empty orbitals on the imido bonds of the active species of complexes 1 and 4 compared to 2 and 3. By comparing the LUMOs of Figure 3 with Figure S59, we can infer that in both cases the empty orbitals with the lowest energy are partially delocalized on the imido bond and a possible reaction with a nucleophile will occur in both the catalyst precursor and in the activated species.

2.3. Ethylene polymerization with MAO

Table 2 shows the polymerization results by complexes 1, 2, 3 and 4 activated by MAO (Al/Ti = 1000) under controlled temperature of 10 °C with ethylene pressure of 2 bar for 60 min. In the synthesized catalysts. After mixing the complex with co-catalyst MAO, color change are observed in complex 1 and 2 from deep red to green in few minutes, while complex 3 and 4 retain the reddish color during the activation time. Complex 4 shows the highest yield and the catalytic activity is $3950 \text{ Kg}_{\text{PE}} \cdot \text{mol}_{\text{Ti}}^{-1} \cdot \text{h}^{-1} \cdot \text{bar}^{-1}$, compared to the other synthesized catalysts. Secondly, complex 3 also shows very high catalyst activity; while complexes 1 and 2 show very limited catalyst activity toward the polymerization of ethylene. Previous find-

Run	Complex ^[a]	Yield [g]	Catalytic activity [$\text{Kg}_{\text{PE}} \cdot \text{mol}_{\text{Ti}}^{-1} \cdot \text{h}^{-1} \cdot \text{bar}^{-1}$]
1	1	0.7	20
2	2	0.3	10
3	3	30.0	1100
4 ^[a]	4	51.8	3950

[a] Polymerization conditions: ethylene pressure = 2 bar, temperature = 10 °C, reaction time = 60 min, Solvent = 750 mL toluene, catalyst = 14 μmol , Al/Ti = 1000 (MAO (10 wt%.sol) (80% vol./vol. scavenger, 20% vol./vol. catalyst activator)). [b] Polymerization results from reference [30].

ings attribute the lower catalyst activity of *ortho*-substituted FI catalysts to a steric hindrance that suppresses the polymerization, while for complex 4 electron withdrawing effect of the fluorines makes the titanium more electrophilic, overcoming the polymerization suppression.^[7] Moreover, because of higher electron-withdrawing effect of fluorine atom, the titanium center of complex 1 is more electrophilic compared with complex 2; therefore, complex 1 has higher catalytic activity than complex 2.

The values of M_w and PDI are estimated from oscillatory frequency sweep data (S48–49) obtained by rheology measurement of the polymers. The results are summarized in Table S47. It shows an increasing M_w of polymers synthesized by complexes 3, 2, 1 and 4, in order. Because of the interaction between F atoms on the ligands and the β -hydrogen (β -H) of the polymer chains (or Ti) the β -H transfer to titanium center is probably disfavored,^[3] resulting in higher molecular weight polyethylene. As previously calculated,^[7] the distance between F and β -H will decrease with increasing number of F atoms in the phenoxyimine ligand. It may cause weaker F–H (or F–Ti) interaction in complex 1, which leads a lower M_w in run 1 compared to run 4. On the other hand, the methyl group is larger than a H atom, so the methyl groups provide more steric pressure than the H atom for preventing β -H termination, which results in the higher molecular weight of run 2 compared with run 3. Compared to run 2, with a similar size of fluorine atom and methyl group, run 1 shows a higher M_w , which is contributed by the influence of F atoms on stabilizing β -H transfer. Run 4 shows much higher M_w than run 3, due to a stronger interaction between the β -H and the fluorine atoms of complex 4. Surprisingly, it seems that there is a relationship between the Mulliken charges on the nitrogen of the catalyst precursors as well as the activated species and the molecular weight of the polymer produced (Figure S60). As the nitrogen bears a more positive charge, the molecular weight increases. These results suggest that the control on the molecular weight of the ligand is a subtle balance of steric and electronic effect. The PDI values of the polymers synthesized exhibits high values, which shows non-living polymerization character reflecting the long polymerization times.

In the above discussion, steric and electronic effects have been considered to explain the catalytic activity data in agreement with previous findings; however, catalyst activations are not included in the discussion and might play a critical role in explaining the differences in the catalytic activity of the complexes synthesized. In particular, in our research group, we have observed a decrease in the catalytic activity when complex 4 is activated with MAO upon long activation times due to the ligand transfer to the TMA in equilibrium with the MAO.^[18,28–29,31–32] On the contrary, for some catalysts, TMA can effectively take part in the activation process.^[13] By using BHT to trap the free TMA we can elucidate the effect of TMA on the complexes synthesized.

FT-IR of the polymer produced (Figures S36–S38) show only the expected classic bands of PE, indicating that the polymers are linear within the sensitivity of the measurements. It needs to be pointed out that the polymers of runs 1–2 contain higher

amount of catalytic ashes which can influence the rheological response of the polymers and, consequently, the estimation of the molecular weight and distribution.

2.4. Ethylene polymerization with MAO/BHT

Table 3 summarizes the polymerization data when the complexes 1–4 are activated with MAO + BHT. After mixing complex with MAO/BHT, no color change is found and the catalytic solution shows reddish.

According to the reported data, the polymerization activity of complex 3 does not change when BHT is used in combination with MAO. Previous reports already showed an increase in the catalyst activity for complex 4 when BHT is used in combination with MAO.^[14,21,30] This difference between complexes 3 and 4 suggests that the TMA does not deactivate the catalyst as rapidly as for complex 4, most likely due to a higher electron density in complex 3 on the Ti metal center. On the contrary, the polymerization by the synthesized complexes 1 and 2 decreases significantly when the activation is performed with MAO/BHT. It could be argued that the TMA assists the activation of the complex to the monoalkylated or active form.

It needs to be taken into consideration that by removing the TMA from the polymerization mix, also a powerful scavenger of the impurities has been removed, making complexes 1 and 2 more susceptible to catalyst poisoning. However, a possible difference in reactivity of the complexes towards a hypothetical unreacted BHT in solution cannot be

fully ruled out. In this scenario, complexes 1 and 2 will be reactive towards BHT (or modified BHT) in solution, while complexes 3 and 4 will not.

FT-IR of the polymer produced (Figures S39–41) show only the expected bands for PE indicating the synthesis of linear chains within the sensitivity of the measurements.

2.5. Ethylene polymerization with DEAC and DEAC + MAO/BHT

To modify the Lewis acidity of the activator, DEAC was used in the activation step. DEAC has lower Lewis acidity compared with TMA, yet higher in comparison to MAO, assumed to be a stronger catalyst activator than MAO. Moreover, to gain further insights in the effect of the catalyst poisoning without the scavenger (TMA), the use of MAO + BHT during the catalyst activation and DEAC used as scavenger has been tested. Table 4 shows the polymerization results. The catalytic solution consisting of complex 3 and DEAC immediately changes from reddish to dark color, however, others keep red color. It is similar as the catalytic solution containing complex 3 with DEAC + MAO/BHT.

Analyzing the data of Table 4 it is striking how the catalyst activity for complexes 1 and 2 double when DEAC is used as catalyst activator proving it to be a better co-catalyst compared with MAO; while complex 3 is inactive and for 4 decreases significantly by more than 2 orders of magnitude. It is also of importance to notice the color of the four complexes; in particular, for complexes 1 and 2 the color remained deep red upon addition of DEAC; while for complex 3 the color changed into dark green. Previous findings reported a reduction of Ti (IV) to Ti (III) in complex 4 for similar conditions when activated with DEAC.^[16] Therefore, by combining the color observation and the polymerization data, the complexes seem to react differently with DEAC; in particular, complexes 1 and 2 seem to be more active when DEAC is used as co-catalyst, while catalyst deactivation processes seem to occur for complexes 3 and 4 with the same co-catalyst as suggested by the color change.

When the polymerization was conducted using the co-catalyst system DEAC + MAO/BHT, the polymerization activity decreases significantly and similar value as the result from the activation with MAO/BHT (Table 3) is obtained for complexes 1 and 2. This suggests that the hypothesis of an interaction

Table 3. Polymerization results of the catalysts with MAO/BHT.

Run	Complex ^[a]	Yield [g]	Catalytic activity [Kg _{PE} *mol _{Ti} ⁻¹ *h ⁻¹ *bar ⁻¹]
5	1	0.03	1
6	2	0.06	2
7	3	29.8	1050
8 ^[b]	4	35.0	4900
9 ^[b]	4	27.0	4000

[a] Polymerization conditions: ethylene pressure = 2 bar, temperature = 10 °C, reaction time = 60 min, Solvent = 750 mL toluene, catalyst = 14 μmol, Al/Ti = 1000 (MAO, 80% vol./vol. MAO/BHT as scavenger, 20% vol./vol. MAO/BHT as catalyst activator. [b] Polymerization results from reference [14].

Table 4. Polymerization results of the catalysts with DEAC and DEAC + MAO/BHT.

Run	Complex ^[a]	Co-catalyst ^[b]	Yield [g]	Catalytic activity [Kg _{PE} *mol _{Ti} ⁻¹ *h ⁻¹ *bar ⁻¹]
10	1	DEAC	0.86	50
11	2	DEAC	0.32	20
12	3	DEAC	Traces	–
13 ^[c]	4	DEAC	–	24
14	1	DEAC + MAO/BHT	0.03	1
15	2	DEAC + MAO/BHT	0.07	2
16	3	DEAC + MAO/BHT	15.30	550

[a] Polymerization conditions: ethylene pressure = 2 bar, temperature = 10 °C, reaction time = 60 min, Solvent = 750 mL toluene, catalyst = 14 μmol, Al/Ti = 1000. [b] When DEAC is used, 80% vol./vol. as scavenger, 20% vol./vol. as catalyst activator. When DEAC + MAO/BHT is used, pure DEAC is used as scavenger while the catalyst is mixed with 50% mol/mol DEAC and 50% mol/mol pre-reacted MAO/BHT. [c] Polymerization results from reference [16].

between the MAO (or BHT) and the catalyst advanced before still cannot be completely ruled out. In contrast, the hypothesis of the absence of a scavenger in the case of MAO/BHT can be ruled out for complexes **1** and **2** because, in runs 14 and 15, DEAC was used as a scavenger for the impurities. Interestingly, complex **3** activated with a (50%–50%) mix of DEAC + MAO/BHT shows reasonably good catalyst activity compared with the activation of DEAC and half the catalyst activity compared with the activation with MAO and MAO/BHT. This result suggests that half of the catalyst is deactivated with DEAC; while the other half is properly activated by the MAO.

FT-IR of the polymer produced (Figures S42–S46) show only the expected classic bands of PE, indicating that the polymers are linear within the sensitivity of the measurements.

2.6. ^1H NMR study of activation with alkyl aluminum

To elucidate the possible change in the different complexes upon activation with common co-catalysts (TEA and TiBA) used routinely, a ^1H NMR study was conducted. It was previously reported, by Li *et al.*, that complex **4** with five fluorine atoms in the phenoxyimine ligand is not efficiently activated in the presence of TEA and TiBA under any circumstances.^[16] This NMR analysis aims to account for the inactivity of the catalyst in the presence of these aluminum alkyls and provide insight into the species generated. Varying combinations of Al/Ti ratio and amounts of pre-catalyst were implemented.

In an ideal activation, the active species of the catalyst would give rise to the same proton signals as the catalyst precursors (perhaps with a slight chemical shift) and a new set of signals arising from the substitution of the chlorines with an

alkyl substituent. However, as both aluminum alkyls are sources of anions, there is a possibility for these to act as nucleophiles and interact with the ligand framework. To recall, the DFT study showed the LUMO to be located on the imino bond, suggesting the energetically most accessible reactivity in the presence of an anionic source. It needs to be mentioned that due to practical restrictions, it is not possible to use the same Al/Ti molar ratio as the one used during the catalysis for NMR measurements. The maximum Al/Ti = 100 gave NMR spectra with an overbearing signal arising from the co-catalyst and no signals were visible from the activated catalyst species (Figure S22–24). Hence, the ratio was lowered, giving improved spectra from which the majority of signals were distinguishable.

In the catalytic system containing a Al/Ti = 1 ratio between complex **2** and co-catalyst TEA, the spectrum as seen in Figure 4 below was obtained. It can be seen that the signal at 8.48 ppm (circled in red) belonging to the N=CH of the imido bond disappears in the presence of TEA, while two new aliphatic signals appear at 0.85 and 0.68 ppm (squared in blue). This suggests that the reaction of C_2H_5^- has taken place with the ligand. A slight change in the chemical shifts to lower ppm values is observed. Furthermore, only one set of signals can be seen, indicating that there is one single ligand framework present, and both ligands on complex **2** have reacted with the TEA.

Similarly, in the equivalent reaction of TEA with complexes **1** and **3** (Figure S25, S26), there are two new aliphatic peaks around 0.66 and 0.85 ppm, at almost equivalent chemical shifts as discerned for complex **2**, implying similar reaction has taken place. The disappearance of the imino hydrogen at 8.48 ppm and the appearance of two new peaks in the aliphatic region at 0.68 and 0.85 ppm are a strong suggestion that the imido bond

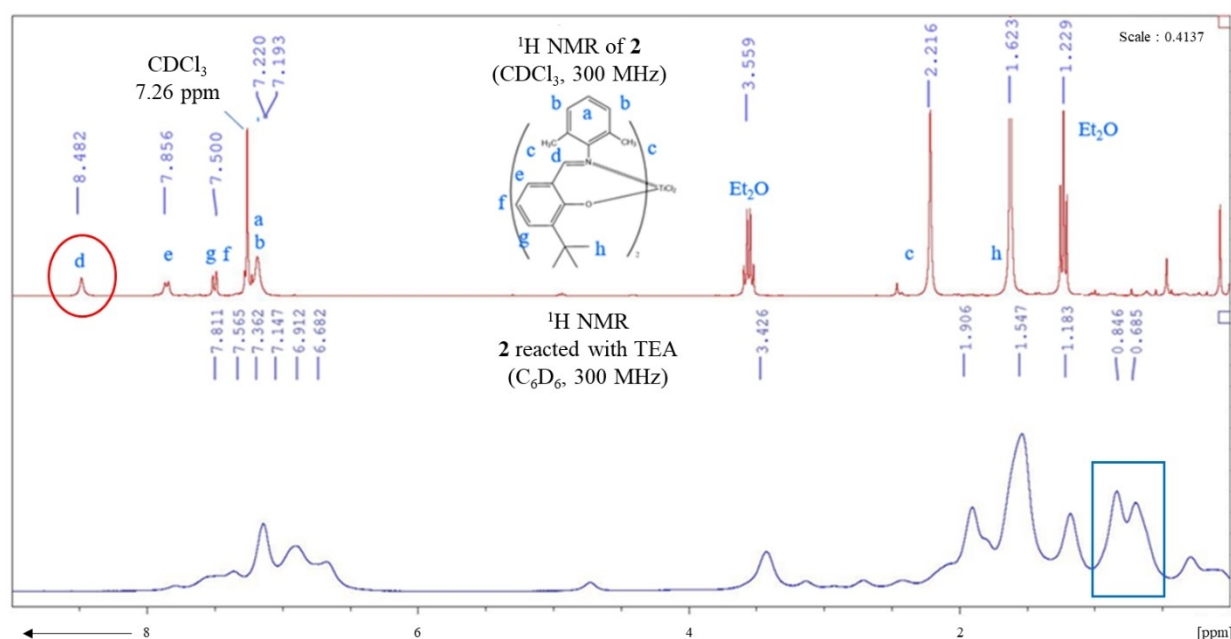
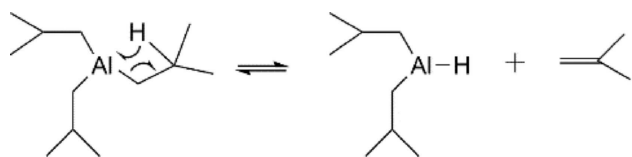


Figure 4. ^1H NMR Spectrum comparison of complex **2** (top) and activated catalyst **2** by TEA in Al/Ti = 1 ratio (bottom).

of the ligand reacts with the ethyl group of the TEA leading to an amine. These results are corroborated with the DFT studies which locate the LUMOs of the four complexes on the imido bonds, predicting the electrophilic position available for a nucleophilic attack.

In ^1H NMR spectra of complexes **1** and **2** with TiBA with Al/Ti = 1 (Figure S27, S28), no distinguishable peaks are visible and the shape of the signals resemble a paramagnetic spectrum. Notably, upon addition of TiBA to the catalysts, a color change to green was observed. This observations strongly suggest a reduction of Ti(IV) to Ti(III) produced by reaction with the TiBA. Previous findings proposed the deactivation of complex **4** in the presence of TMA, leading to a Ti(III) complex.^[15,28–29] Nevertheless, ^1H NMR spectrum (Figure S29) of complex **3** reacted with TiBA shows the absence of the peak around 8 ppm ($-\text{N}=\text{CH}-$), while a new peak around 4.5 appears. It may be due to the reaction between H^- and $-\text{N}=\text{CH}-$ forming $\text{N}-\text{CH}_2-$. The hydride can be generated upon β -hydrogen elimination in the TiBA generating a di-*iso*-butylaluminum hydride,^[34–37] as Scheme 2.

It is expected that if a reaction occurs with the ligand, it will generate a species where the double bond between the

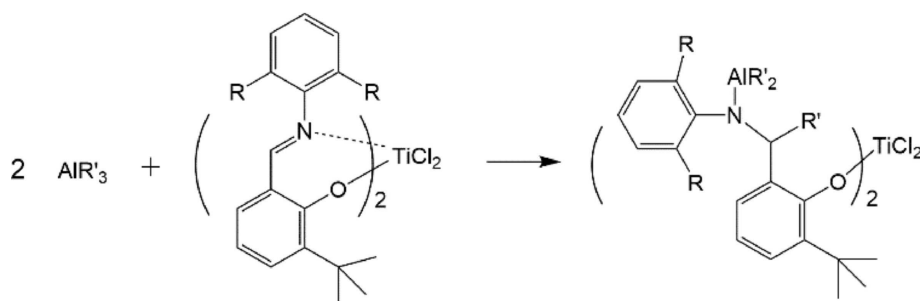


Scheme 2. The formation of H^- from TiBA.

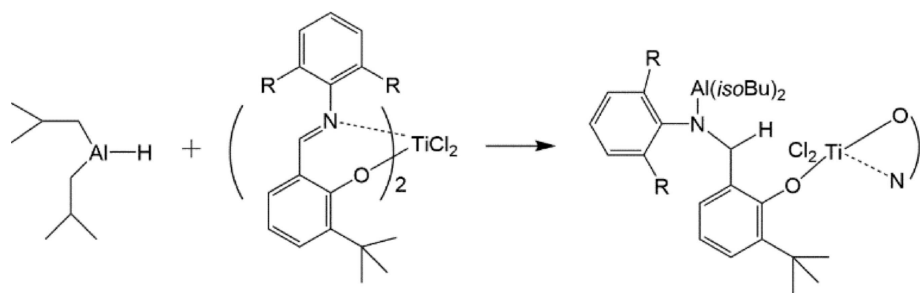
nitrogen and carbon is lost, as this is the strongest electrophile in the ligand framework. The carbon will bind to an H^- or a C_2H_5^- generated as anions from TiBA and TEA respectively. The coordinative bond initially observed between Ti–N will now be of higher covalent nature. The signal at approximately 8 ppm ($-\text{N}=\text{CH}-$) shifts much further upfield due to the transition of an imine to an amine, and give a second aliphatic signal from the H or ethyl at lower chemical shifts. The predicted reaction is summarized in Scheme 3. A similar scheme for TiBA has been proposed to describe the reactivity of bis(pyrrrolideimine)-based catalysts.^[38]

These results provide experimental NMR evidence of the reaction of the TEA and TiBA to bis(phenoxyimine)TiCl₂ catalysts. The outcome of the NMR study corroborates with previous findings where a bis(phenoxyimine)ZrCl₂ reacted with TiBA followed by hydrolysis yielding a phenoxyamine moiety.^[39] To further support the reactivity of complexes **1** to **4** with TiBA, energetics of the reaction has been calculated using DFT calculations. The reaction considered is depicted in Scheme 4 which can be considered a mix of Schemes 2 and 3. Due to the long computational demand of the DFT calculations, only one ligand is considered to react with TiBA. However, one ligand modification is sufficient to irreversibly change the catalytic properties of complexes **1–4**.

For all the complexes investigated, the energy difference (Table S61) is in a range between -27 and -35 Kcal/mol, supporting the favor thermodynamic driving force of the reaction depicted in scheme 4. A short distance between the F...Al is calculated (2.160 Å for complex **1** and 2.247 Å for complex **4**), indicating an interaction between the two atoms.



Scheme 3. Generation of new species for complexes **1** (R=F) and **2** (R=CH₃) resulting from the reaction with TEA (R'=CH₂CH₃) and TiBA (R'=CH₂CH(CH₃)₂) or 2x CH₂CH(CH₃)₂ with 1x H where H is transferred to the ligand).



Scheme 4. Ligand modification promoted by the di-*iso*-butyl aluminum hydride.

We ascribe the lower values of energy for the reaction with TiBA calculated for complexes **1** and **4** to this stabilizing interaction compared with complexes **2** and **3**. Once again, it seems that there is a correlation between the calculated energy differences with the Mulliken charges bore by the nitrogens for complexes **1** to **4** (Figure S62). This relationship, together with the observed relationship with the M_w , suggest that electronic effect on the nitrogen is critical in understanding the structure-property relationship of the phenoxyimine complexes.

The discussed ^1H NMR study brought insight into the activity and reactivity of the synthesized complexes with alkylaluminums. It presents the reactivity of the ligand framework in the presence of anionic sources, and elucidates rationale for the published catalytic inactivity of FI catalysts with TEA and TiBA.^[16] Phenoxyamine Ti(IV) catalysts are reported to be significantly less active in the polymerization of ethylene compared with phenoxyimine Ti(IV) addressing also for the observed poor catalytic activity of complexes **1** and **2** compared with complexes **3** and **4**.

3. Conclusions

The synthesized complexes **1** (difluoro) and **2** (dimethyl), showed reducing catalytic activity with co-catalyst MAO for ethylene polymerization when compared with complexes **3** and **4**. It proves that the *ortho*-groups (F and CH_3) of the N-phenyl in the ligand will suppress the ethylene polymerization with a bulky co-catalyst. Higher electron-withdrawing fluorine atoms in complex **4** enhances the electrophilic property of metal Ti resulting in a higher catalytic activity. The activation with different co-catalysts (MAO/BHT, DEAC, DEAC+MAO/BHT) with complexes **1** and **2** displayed a decreasing activity order following $\text{DEAC} > \text{MAO} > \text{DEAC} + \text{MAO/BHT} = \text{MAO/BHT}$. It suggests that the residual TMA in MAO solution plays a crucial role in the catalyst activation for complexes **1** and **2**, while the absence of TMA in MAO does not play a significant role for complex **3**. Surprisingly, when complex **3** is activated with DEAC a color change is observed with catalyst deactivations; this suggests the appearance of the reduction of Ti(IV) to Ti(III). Furthermore, the activation study of complexes **1**–**3** by NMR suggests the generation of Ti(III) by reducing Ti(IV) with TiBA, showing a paramagnetic character of ^1H NMR spectra and color change of the catalyst solution. When the complexes **1** and **2** meet with TEA, the ^1H NMR spectrum showed two new aliphatic peaks around 0.66 and 0.85 ppm while absented the peak around 6.5–8.3 ppm of aromatic protons. These results suggests that anionic source from TEA may interact with N=C bond forming C–R bond (R represent Ethyl for TEA or H for TiBA), and this is similar as complex **3** activated with TEA and TiBA giving account for previously published inactivity results. These results are potentially applicable to all imine-based ligand complexes activated with aluminum alkyls for olefins polymerization. Surprisingly, it seems that there are almost liner relationship between M_w or the calculated energy from the reaction of TiBA with the complexes and the nitrogen Mulliken charge. These unexpected results suggest that the overlooked electronic

effect on the nitrogen plays a critical role. The alteration of *ortho* substituents on the phenoxyimine ligands in FI complexes has proven a necessary balance between steric and electronic effects, whilst the investigation into co-catalyst systems highlights the different effects on the activation of the catalyst precursors.

Acknowledgments

This research has been made possible with the support of the Dutch province of Limburg and the China Scholarship Council (CSC201808330427).

Conflict of Interest

The authors declare no conflict of interest.

Keywords: Activation · Alkylaluminum · DFT · FI catalysts · UHMWPE

- [1] H. Makio, H. Terao, A. Iwashita, T. Fujita, *Chem. Rev.* **2011**, *111*, 2363.
- [2] S. Matsui, T. Fujita, *Catal. Today* **2001**, *66*, 63.
- [3] H. Makio, N. Kashiwa, T. Fujita, *Adv. Synth. Catal.* **2002**, *344*, 477.
- [4] M. Mitani, J. Saito, S. Ishii, Y. Nakayama, H. Makio, N. Matsukawa, S. Matsui, J. Mohri, R. Furuyama, H. Terao, H. Bando, H. Tanaka, T. Fujita, *Chem. Rec.* **2004**, *4*, 137.
- [5] H. Makio, T. Fujita, *Acc. Chem. Res.* **2009**, *42*, 1532.
- [6] S. Matsui, M. Mitani, J. Saito, Y. Tohi, H. Makio, H. Tanaka, T. Fujita, *Chem. Lett.* **1999**, 1263.
- [7] M. Mitani, J. Mohri, Y. Yoshida, J. Saito, S. Ishii, K. Tsuru, S. Matsui, R. Furuyama, T. Nakano, H. Tanaka, S. Kojoh, T. Matsugi, N. Kashiwa, T. Fujita, *J. Am. Chem. Soc.* **2002**, *124*, 3327.
- [8] S. Matsui, M. Mitani, J. Saito, N. Matsukawa, H. Tanaka, T. Nakano, T. Fujita, *Chem. Lett.* **2000**, *29*, 554.
- [9] A. Iwashita, C. W. Chan Michael, H. Makio, T. Fujita, *Catal. Sci. Technol.* **2014**, *4*, 599.
- [10] M. P. Weberski Jr., C. L. Chen, M. Delferro, C. Zuccaccia, A. Macchioni, T. J. Marks, *Organometallics* **2012**, *31*, 3773.
- [11] M. P. Weberski Jr., C. L. Chen, M. Delferro, T. J. Marks, *Chem. Eur. J.* **2012**, *18*, 10715.
- [12] D. Romano, *PhD thesis*, Loughborough University (UK) **2014**.
- [13] H. X. Zhang, Y. Lee, J. Park, D. Lee, K. Yoon, *J. Appl. Polym. Sci.* **2011**, *120*, 101.
- [14] D. Romano, E. Andablo-Reyes, S. Ronca, S. Rastogi, *Polymer* **2015**, *74*, 76.
- [15] M. Bochmann, *Organometallics* **2010**, *29*, 4711.
- [16] T. Li, F. W. Kong, R. Liu, Z. Y. Li, F. M. Zhu, *J. Appl. Polym. Sci.* **2011**, *119*, 572.
- [17] H. Sinn, W. Kaminsky, H. Vollmer, R. Woldt, *Angew. Chem. Int. Ed. Engl.* **1980**, *19*, 390.
- [18] D. W. Imhoff, L. S. Simeral, S. A. Sangokoya, J. H. Peel, *Organometallics* **1998**, *17*, 1941.
- [19] H. Sinn, *Macromol. Symp.* **1995**, *97*, 27.
- [20] According to the certificate of analysis from Albemarle, approximately 1.7 wt% of TMA is present in the MAO 10 wt% toluene solution.
- [21] D. Romano, S. Ronca, S. Rastogi, *Macromol. Symp.* **2015**, *356*, 61.
- [22] H. Makio, T. Fujita, *Macromol. Symp.* **2004**, *213*, 221.
- [23] K. P. Bryliakov, E. A. Kravtsov, D. A. Pennington, S. J. Lancaster, M. Bochmann, H. H. Brintzinger, E. P. Talsi, *Organometallics* **2005**, *24*, 5660.
- [24] V. Busico, R. Cipullo, F. Cutillo, N. Friederichs, S. Ronca, B. Wang, *J. Am. Chem. Soc.* **2003**, *125*, 12402.
- [25] M. J. Frisch, G. W. Trucks, H. B. Schlegel, G. E. Scuseria, M. A. Robb, J. R. Cheeseman, G. Scalmani, V. Barone, B. Mennucci, G. A. Petersson, H. Nakatsuji, M. Caricato, X. Li, H. P. Hratchian, A. F. Izmaylov, J. Bloino, G. Zheng, J. L. Sonnenberg, M. Hada, M. Ehara, K. Toyota, R. Fukuda, J.

- Hasegawa, M. Ishida, T. Nakajima, Y. Honda, O. Kitao, H. Nakai, T. Vreven, J. A. Montgomery, J. E. Peralta, F. Ogliaro, M. Bearpark, J. J. Heyd, E. Brothers, K. N. Kudin, V. N. Staroverov, T. Keith, R. Kobayashi, J. Normand, K. Raghavachari, A. Rendell, J. C. Burant, S. S. Iyengar, J. Tomasi, M. Cossi, N. Rega, J. M. Millam, M. Klene, J. E. Knox, J. B. Cross, V. Bakken, C. Adamo, J. Jaramillo, R. Gomperts, R. E. Stratmann, O. Yazyev, A. J. Austin, R. Cammi, C. Pomelli, J. W. Ochterski, R. L. Martin, K. Morokuma, V. G. Zakrzewski, G. A. Voth, P. Salvador, J. J. Dannenberg, S. Dapprich, A. D. Daniels, O. Farkas, J. B. Foresman, J. V. Ortiz, J. Cioslowski, D. J. Fox, *Gaussian 09*, Gaussian Inc.: Wallingford (USA) **2004**.
- [26] D. W. Mead, *J. Rheol.* **1994**, *38*, 1797.
- [27] J. Saito, M. Mitani, S. Matsui, Y. Tohi, H. Makio, T. Nakano, H. Tanaka, N. Kashiwa, T. Fujita, *Macromol. Chem. Phys.* **2002**, *203*, 59.
- [28] K. P. Bryliakov, N. V. Semikolenova, V. A. Zakharov, E. P. Talsi, *J. Organomet. Chem.* **2003**, *683*, 23.
- [29] K. P. Bryliakov, E. A. Kravtsov, D. A. Pennington, S. J. Lancaster, M. Bochmann, H. H. Brintzinger, E. P. Talsi, *Organometallics* **2005**, *24*, 5660.
- [30] D. Romano, N. Tops, E. Andablo-Reyes, S. Ronca, S. Rastogi, *Macromolecules* **2014**, *47*, 4750.
- [31] A. R. Barron, *Organometallics* **1995**, *14*, 3581.
- [32] L. Resconi, S. Bossi, L. Abis, *Macromolecules* **1990**, *23*, 4489.
- [33] A. Laine, M. Linnolahti, T. A. Pakkanen, *J. Organomet. Chem.* **2012**, *716*, 79.
- [34] G. Giacomelli, A. M. Caporusso, L. Lardicci, *Tetrahedron Lett.* **1981**, *22*, 3663.
- [35] A. M. Caporusso, G. Giacomelli, L. Lardicci, *J. Org. Chem.* **1982**, *47*, 4640.
- [36] L. E. Overman, R. J. McCready, *Tetrahedron Lett.* **1982**, *23*, 2355.
- [37] M. Bochmann, *Organometallics and Catalysis: An Introduction*, Oxford University Press **2015**, P. 47.
- [38] T. Matsugi, T. Fujita, *Chem. Soc. Rev.* **2008**, *37*, 1264.
- [39] S. Matsui, M. Mitani, J. Saito, Y. Tohi, H. Makio, N. Matsukawa, Y. Takagi, K. Tsuru, M. Nitabarau, T. Nakano, H. Tanaka, N. Kashiwa, T. Fujita, *J. Am. Chem. Soc.* **2001**, *123*, 6847.

Manuscript received: April 29, 2020
Revised manuscript received: June 29, 2020
Accepted manuscript online: July 2, 2020
Version of record online: September 8, 2020